Nuclear Engineering and Technology 49 (2017) 1752–1757

Contents lists available at ScienceDirect

Nuclear Engineering and Technology

journal homepage: www.elsevier.com/locate/net

Original Article

Analysis of radioactivity levels and hazard assessment of black sand samples from Rashid area, Egypt

Mohamed A.E. Abdel-Rahman [a, *], Sayed A. El-Mongy [b]

[a] Nuclear Engineering Department, Military Technical College, Kobry El-kobbah, Cairo, Egypt
[b] Nuclear and Radiological Regularity Authority (ENRRA), Ahmed Al-Zomer Street, P.O. Box 7551, Nasr City, Cairo, Egypt

ARTICLE INFO

Article history:
Received 20 February 2017
Received in revised form
15 July 2017
Accepted 25 July 2017
Available online 15 August 2017

Keywords:
Black Sand
Environmental Impact
Gamma Spectrometry
Radioactivity Levels
Radiological Hazards Assessment

ABSTRACT

The aim of this study is to evaluate the radioactivity levels and radiological impacts of representative black sand samples collected from different locations in the Rashid area, Egypt. These samples were prepared and then analyzed using the high-resolution gamma ray spectroscopy technique with a high-purity germanium detector. The activity concentration (A_c), minimum detectable activity, absorbed gamma dose rate, external hazard index (H_{ex}), annual effective dose rate equivalent, radium equivalent, as well as external and internal hazard index (H_{ex} and H_{in}, respectively) were estimated based on the measured radionuclide concentration of the ^{238}U(^{226}Ra) and ^{232}Th decay chains and ^{40}K. The activity concentrations of the ^{238}U, ^{232}Th decay series and ^{40}K of these samples varied from 45.11 ± 3.1 Bq/kg to 252.38 ± 34.3 Bq/kg, from 64.65 ± 6.1 Bq/kg to 579.84 ± 53.1 Bq/kg, and from 403.36 ± 20.8 Bq/kg to 527.47 ± 23.1 Bq/kg, respectively. The activity concentration of ^{232}Th in Sample 1 has the highest value compared to the other samples; this value is also higher than the worldwide mean range as reported by UNSCEAR 2000. The total absorbed gamma dose rate and the annual effective dose for these samples were found to vary from 81.19 nGy/h to 497.81 nGy/h and from 99.86 μSv/y to 612.31 μSv/y, which are higher than the world average values of 59 nGy/h and 70 μSv/y, respectively. The H_{ex} values were also calculated to be 3.02, 0.47, 0.63, 0.87, 0.87, 0.51 and 0.91. It was found that the calculated value of H_{ex} for Sample 1 is significantly higher than the international acceptable limit of <1. The results are tabulated, depicted, and discussed within national and international frameworks, levels, and approaches.

1. Introduction

There are naturally occurring radioactive series that have been in existence since the earth was created. Each of these is headed by a very long-lived parent such as ^{238}U (4.5×10^9 years) and ^{232}Th (1.39×10^9 years). In each chain, the nuclides decay by emitting α or β particles until stable lead is reached [1]. As a matter of fact, different locations worldwide are naturally rich in uranium or thorium minerals. Based on International Atomic Energy Agency (IAEA) publications, the highest known reserves of thorium are contained in the beach and inland placer deposits of monazite, a mixed phosphate mineral; Egypt has potential and feasible estimated thorium reserves [2]. The Rashid area in Egypt is considered a promising site with high abundance of black sand monazite minerals [3].

Nondestructive technique gamma spectrometry is an effective and essential tool to analyze different materials and matrices containing natural and/or anthropogenic radionuclides. The concept of dose equivalent and external hazard index is used to assess radiological hazard for different kinds of radiation of various radionuclides.

2. Materials and methods

2.1. Sample preparation

Seven representative sand samples were investigated in this study. These samples were collected from seven different locations along the Rashid city coast, which has an area of 2.5 km^2. The samples collected in this work are part of a comprehensive plan to evaluate the monazite deposits and thorium content in the Rashid area. The target of this plan necessitates collection of hundreds of samples based on a systematic approach. Homogeneity and representative nature of samples analyzed in this study reflect a

* Corresponding author.
E-mail address: mabdelrahman@mtc.edu.eg (M.A.E. Abdel-Rahman).

http://dx.doi.org/10.1016/j.net.2017.07.020

scientific sampling mechanism and justify the number of representative samples used.

The samples were collected from the top surface layers and then packed in labeled plastic bags with date and location; they were then transported to the nuclear spectroscopy laboratory in Cairo for analysis.

The collected samples were dried in a drying oven at 90°C for 24 h to remove the moisture. Subsequently, the samples were crushed into fine powder and then sieved using a 2 mm mesh to obtain a uniform particle size. Each sample was weighed after sieving. The meshed samples were then transferred to 100-mL Marinilli containers, which were sealed with polyvinyl chloride insulation tape. For natural radioactivity level measurements of these samples, they were kept undisturbed for 1 month (typically 28 days, representing 7 half-lives of ^{222}Rn) prior to analysis to attain radioactive secular equilibrium between ^{226}Ra (the ^{238}U decay chain) and the ^{232}Th series and their daughters. Once this time had elapsed, the activity of ^{226}Ra and its daughters were equal. Finally, to achieve good counting statistics, the gamma decay spectra from the samples were measured for 86,400 s (24 h).

2.2. Measurement arrangement

In this study, black sand samples were analyzed using the high-resolution gamma ray spectroscopy technique with a high-purity germanium (HpGe) detector of ~50% efficiency. The HpGe detector (Canberra), with its built-in preamplifier, is operated with a high voltage power supply at approximately 3 MeV. For cooling, the germanium crystal was fully immersed in liquid nitrogen through a cryostat to reduce the noise of leakage current. The output signal was connected to a spectroscopy shaping amplifier, followed by a multi-channel analyzer with 8,192 channels. The shaping time was adjusted to 8 microseconds, and the fine gain and course gain were set at 0.64 and 10, respectively. Finally, the spectra of all samples and standard sources were analyzed using Genie 2000 software (Canberra). The detailed specifications of the HpGe detector are given in Table 1.

The HpGe detector was shielded against sources of surrounding background radiation, such as natural radionuclides in building materials including ^{40}K, cosmic rays, and uranium decay series nuclides, by a thick lead case with a fixed base and movable cover. Special consideration was taken for the decay products of the naturally occurring isotopes of uranium (^{238}U of 99.275% and ^{235}U of 0.720% natural abundance), thorium (^{232}Th), and potassium (^{40}K).

All experiments were performed twice for verification, with one experiment carried out in the nuclear engineering department at the Military Technical College and the second performed at the Nuclear & Radiological Regulatory Authority laboratory. The reference IAEA sample (S16) with the same geometry as that of the analyzed samples, and well known activities, was used for verification and validation of the results. This reference material (IAEA-S16 of 1.68 wt.% for Th and 445 μg/g for U) was used for quality control. The measured and calculated S16 activities were in very good agreement with the IAEA-certified values.

Table 1
Technical specifications of HpGe detector used in this study.

Detector model	GC5019
Preamplifier model	2002CSL
Cryostat model	7500SL
Relative efficiency	≥50%
Resolution	≤1.9 keV @ 1.33 MeV
Endcap size	3.25 inches (diameter)
Endcap length	5.75 inches (length)
Diameter	65.7 mm
Length	63.4 mm
Distance from window	5.71 mm

HpGe, high-purity germanium.

In order to measure the background distribution values for the HpGe detector, a Marinelli container filled with deionized water, and with a shape identical to the sample, was placed on the top of the detector and counted. All measurements for both background and black-sand samples and the reference have the same counting time, 86,400 s (24 h). The spectra of all samples and standard sources were collected using Genie software in the same way and with the same geometry as was done for the background counting.

The performance of the radioactivity measurements depends on certain parameters of the system setup. In this study, the energy and efficiency calibration of the HpGe spectrometer are of significant importance to ensure the accuracy of the spectrum analysis and the accuracy of the results. So, the next step was to calibrate the HpGe detector used in this work.

2.3. Detector characteristics

2.3.1. Energy calibration

Energy calibration of the HpGe detector system is performed to obtain a relationship between the channel number of the peak position in the spectrum and the corresponding gamma ray energy. This kind of calibration was performed using standard sources of ^{60}Co, ^{137}Cs, and ^{152}Eu, with activities of 1 μCi each and with multiple photopeaks of known energies. The standard sources are in an energy range of 121–1,407 keV. The standard sources are placed on the top of the HpGe detector, and detector spectrum was obtained with a counting time of 1,200 s (20 min) to obtain high counts with good statistics.

By using standard sources with known activity and gamma ray energies, a plot between the channel number and the energy was obtained using the following linear equation:

$$\text{Energy (keV)} = 0.333 \times \text{Channel} + 2.062 \quad (1)$$

The identification of radionuclides occurring in background and black sand samples can then be achieved based on their energies.

2.3.2. Efficiency calibration

The absolute photopeak efficiency, which depends on the source-detector geometry and the gamma energy, was measured. The absolute full-energy peak efficiency of the HpGe detector can be calculated using the following equation [4]:

$$\varepsilon_{abs} = \frac{C_t}{N_\gamma} \times 100\%, \quad (2)$$

where C_t is the total number of counts recorded per unit time. N_γ is the number of gamma quanta emitted by the source per unit time and can be calculated by [1]:

$$N_\gamma = D_s I_\gamma(E_\gamma), \quad (3)$$

where D_s is the certified activity or the disintegration rate of the source. $I_\gamma(E_\gamma)$ is the branching ratio or the fractional number of gamma rays emitted per disintegration. The efficiency calibration of the detector is performed using standard IAEA radionuclide sources (Eckert & Ziegler Analytics, Cairo – Egypt, Al-Maadi, Technical and chemical services Co), such as isotope product model S-14 (containing ^{234}U, ^{235}U, and ^{238}U). Using Excel software, the efficiency curve of the detector was plotted versus different photopeak energies, with results shown in Fig. 1. The efficiency curve starting from the 186-keV gamma transition was obtained by polynomial fitting of the data.

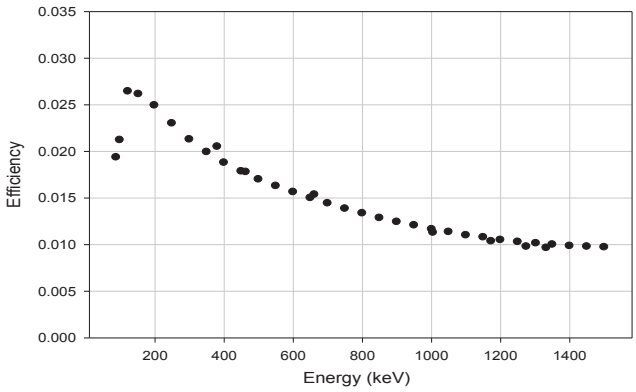

Fig. 1. Efficiency curve of the detector.

Using IAEA standard sources of almost the same structure and geometry as the samples allows the elimination of the effects of variation of the geometry, solid angle (Ω), and sample compositions. In other words, the value of Ω was neglected in these activity calculations.

2.3.3. Background spectrum and minimum detectable activity calculation

When working with low activity samples and measurements of environmental radioactivity, it is necessary to determine the minimum detectable activity (MDA) of the counting system [1]. Environmental background radiation in the detection system can come from different sources. These include 10% of the background created through the device itself, 40% from its immediate environment, 10% from radon in the air, and the remaining 40% from interactions of cosmic rays with the detector and its shield [5].

In this paper, a Marinelli beaker filled with deionized water was used to estimate the background radiation. The Marinelli container of the background sample has the same geometry applied for the black sand samples. Table 2 shows the radionuclides and gamma ray energy peaks of the background spectrum; these are mainly attributable to the ^{238}U, ^{232}Th decay chains and ^{40}K. These peaks reside on a continuum due to Compton scattering of the γ rays and backscattering, the annihilation peak at 511 keV of pair production processes and bremsstrahlung owing to direct interaction of cosmic particles with the detector and shielding material [4].

As mentioned before, when dealing with samples with low radioactivity levels, it is important to calculate the detection limits (L_D) and MDA of the HpGe detection system. The MDA is the smallest amount of radioactive nuclide that can be measured with a certain degree of confidence. The MDA of each radionuclide in a spectrum is calculated from the background spectrum with the same conditions, such as sampling time, geometry, and amplifier gain.

The net count for each nuclide is determined by subtracting the background count from the sample count. Then, both the detection limits and the MDA values of the detection system were calculated using the following equations:

$$L_C = 2.32\sigma_B \tag{4}$$

$$L_D = 2.706 + 4.653\sigma_B \tag{5}$$

$$\mathrm{MDA} = \frac{L_D}{\varepsilon_{abs} \cdot I_\gamma(E_\gamma) \cdot T}, \tag{6}$$

where σ_B is the background counting, ε_{abs} is the absolute photopeak efficiency, $I_\gamma(E_\gamma)$ is the gamma emission probability per decay of the specific peak, and T is the counting time of the sample. The critical level, L_C, is defined as the level above which the net counts present some detected activity with a certain degree of confidence.

Sample spectrum analysis. Black sand samples collected from different locations in Rashid city were measured at the same counting time (86,400 s) and geometry as used for the background and S16 reference samples. Well-resolved peaks of each spectrum were recognized and identified by matching centroid energies with the energy lines in the stored nuclides library. The gamma ray lines of each sample show a wide range of energies from 50 keV up to 2.6 MeV owing to the naturally occurring radioactive materials ^{238}U, ^{232}Th decay series and ^{40}K.

The activity concentration of ^{238}U in the samples was determined using the γ-ray of its decay daughters such as ^{226}Ra, ^{214}Pb, and ^{214}Bi. The activity concentration of ^{232}Th was estimated using all the measured γ-ray transitions related to the decay products such as ^{212}Pb, ^{228}Ac, and ^{208}Tl.

According to the low activity concentration of ^{235}U (0.72% of natural uranium) in the samples, ^{235}U was not identified clearly in all spectra of the samples. On the contrary, ^{40}K (1,460.83 keV) was clearly observed in all the samples and background spectra. Global man-made ^{137}Cs of 661.6 keV was below the detection limits of the system used. Black sand Sample 1 has relatively high counts in all its photo peaks, indicating the high activity concentration of ^{232}Th radionuclide.

3. Results and discussion

3.1. Results of critical level and MDA calculation

The calculated values of critical level (L_C), detection limit (L_D), and *MDA* for each daughter radionuclide of the ^{232}Th and ^{238}U decay series and ^{40}K are illustrated in Table 2.

Table 2
Critical levels, detection limits, and MDA values for the investigated radionuclides.

	Energy (keV)	Branching ratio $I_\gamma(E_\gamma)$	Efficiency (ε)	Background (counts)	Critical level, L_C (counts)	Detection limit, L_D (counts)	MDA (Bq)
Ra-226	186.21	0.0359	0.02885	93 ± 8.27	22.43	47.58	0.53
Pb-214	351.92	0.372	0.02036	65 ± 5.13	18.75	40.22	0.06
Bi-214	609.31	0.463	0.01151	39 ± 2.34	14.53	31.77	0.07
Bi-214	1120.29	0.15	0.00780	22 ± 2.53	10.91	24.53	0.24
Pb-212	238.63	0.446	0.02848	84 ± 5.04	21.32	45.35	0.04
Ac-228	338.40	0.11	0.01765	61 ± 6.98	18.17	39.05	0.23
Ac-228	911.07	0.278	0.00785	31 ± 2.58	12.95	28.61	0.15
Ac-228	968.90	0.17	0.00985	27 ± 3.23	12.09	26.89	0.19
Tl-208	583.10	0.84	0.01310	41 ± 3.19	14.89	32.50	0.03
Tl-208	2614.47	0.997	0.00430	26 ± 1.34	11.86	26.43	0.07
K-40	1460.75	0.106	0.00764	111 ± 6.47	24.51	51.73	0.74

MDA, minimum detectable activity.

It was found that the MDA values for the analyzed samples were in the range 0.06–0.24 for the ^{238}U (^{226}Ra) series, in the range 0.03–0.23 for the ^{232}Th series, and at 0.74 Bq for ^{40}K. The L_C value is used as an indicator for whether the samples have radioactivity. If L_C is higher than the net count of a given sample, it means that there is no significant radioactivity of the considered radionuclide in this sample. Contrarily, if the L_C is less than the net count measured in a sample, this indicates that there is detectable activity in that sample [6].

3.2. Results of activity concentration measurement (A_c)

The activity concentrations (in Bq/kg) of the gamma lines emitted from the daughter nuclides of the ^{238}U, ^{232}Th decay series and ^{40}K in the measured samples were calculated using the following equation:

$$A_C = \frac{C_{net}}{\varepsilon_{abs} \cdot I_\gamma(E_\gamma) \cdot Tm} \quad (7)$$

where C_{net} is the net number of counts in a given peak area corrected from background peaks and m is the mass of the measured sample (kg). Table 3 shows the activity concentration (A_C) values for the seven black sand samples of the selected daughter nuclides of the ^{238}U, ^{232}Th decay series and ^{40}K. The daughter nuclides are assumed to be in secular equilibrium with their parents.

The activity concentration values ranged from 64.65 ± 6.1 Bq/kg to 579.84 ± 53.1 Bq/kg for ^{232}Th; from 45.11 ± 3.1 Bq/kg to 252.38 ± 34.3 Bq/kg for ^{238}U; and from 403.36 ± 20.8 Bq/kg to 527.47 ± 23.1 Bq/kg for ^{40}K. The highest activity concentration values for the ^{238}U and ^{232}Th series were found to be 252.38 ± 34.3 Bq/kg and 579.84 ± 53.1 Bq/kg, respectively, for black sand Sample 1. On the contrary, the lowest values were found to be 45.11 Bq/kg and 64.65 ± 6.1 Bq/kg for Sample 2.

In Sample 1, the activity concentration of ^{232}Th was found to be the highest among the other black sand samples. The variation of activity within the analyzed samples is attributed to the location, as well as to the mineralogy of the collected representative homogenized samples. This variation in activity cannot be attributable to the depth, because all samples were collected at the same depth. Several authors have attributed these variations to either the movement (mobility) or fixation of ^{232}Th in the crystal structure of black sand and its geochemical nature [7–9]. In another study, concerning the Egyptian beach monazite, it was mentioned that the uranium and thorium content of zircon show substantial variation because of the presence of several varieties of beach zircon. The existence of uranium and thorium in zircon is attributable either to defects in the zircon structure or to inclusion of radioactive minerals such as uranothorite [10].

In general, and according to one of IAEA publication, Egypt is counted in the list of countries (Brazil, India, Australia, USA, Canada, Egypt, etc.) that have potentially feasible deposits of thorium [2].

3.3. Results of radiation hazard index calculation

Radiation hazard due to specified radionuclides such as ^{238}U, ^{232}Th, and ^{40}K can be assessed using different indices according to UNSCEAR 2000; this allows us to arrive at a safe conclusion on the health status of an exposed person or environment. The values of either absorbed gamma dose rate ($\dot{D}$), or annual effective dose rate equivalent (AEDRE), or external and internal hazard indices (H_{ex} and H_{in}, respectively) are correlated to the activity concentrations of ^{238}U, ^{232}Th, and ^{40}K for the measured black sand samples, as can be seen in the following equations.

3.3.1. Absorbed gamma dose rate ($\dot{D}$)

The absorbed dose rate ($\dot{D}$, in nGy/h), in the air at 1 m above the ground level can be estimated using the following formula (which is provided by UNSCEAR [5]):

$$\dot{D} = 0.461A_{c(Ra)} + 0.623A_{c(Th)} + 0.0414A_{c(K)} \quad (8)$$

where $A_{c(Ra)}$, $A_{c(Th)}$, and $A_{c(K)}$ are the average activity concentrations of ^{226}Ra, ^{232}Th, and ^{40}K (in Bq/kg), respectively, in the measured samples. For this formula, it is assumed that all the decay products of ^{226}Ra and ^{232}Th are in equilibrium with their parents. Also, as ^{226}Ra contributes about 98% of the total dose, it is replaced with ^{238}U in this formula and, therefore, it makes no difference whether or not if there is an equilibrium between ^{238}U and ^{226}Ra [11–13].

3.3.2. AEDRE and external hazard index (H_{ex})

The concept of dose equivalent and external hazard index is used to assess radiological hazard for different kinds of radiation. The major purpose of these values is to limit the external gamma radiation dose to the admissible dose limit of 1 mSv/y for a "safe" radiation hazard. Because of exposure to γ-rays, the values of both the annual effective dose rate (mSv/y) and the external hazard index (H_{ex}) can be obtained using Eqs. (9) and (10) [7,14,15]:

$$\begin{aligned} \text{AEDRE (mSv/y)} &= \dot{D}\ \text{(nGy/h)} \times 0.7 \times 0.2 \times 8.54 \times 10^{-3} \\ &= \dot{D}\ \text{(nGy/h)} \times 1.23 \times 10^{-3} \end{aligned} \quad (9)$$

$$H_{ex} = \frac{A_{c(U)}}{370} + \frac{A_{c(Th)}}{259} + \frac{A_{c(K)}}{4810} \quad (10)$$

The dose rate data are obtained from the activity concentration values of the natural radionuclides in the measured samples. The factors 0.7 Sv/Gy and 0.2 are the conversion coefficient of air

Table 3
Activity concentrations for the radionuclides of the seven black sand samples.

Radioisotopes	Energy (keV)	Ac-1 (Bq/Kg)	Ac-2 (Bq/Kg)	Ac-3 (Bq/Kg)	Ac-4 (Bq/Kg)	Ac-5 (Bq/Kg)	Ac-6 (Bq/Kg)	Ac-7 (Bq/Kg)
Ra-226	186.21	267.08 ± 14.40	52.58 ± 1.54	69.87 ± 2.66	115.85 ± 6.3	103.38 ± 4.11	48.69 ± 4.11	115.68 ± 6.21
Pb-214	351.92	202.37 ± 9.09	55.33 ± 2.86	60.55 ± 2.89	100.6 ± 3.62	91.93 ± 5.03	41.36 ± 1.88	99.71 ± 3.36
Bi-214	609.31	252.56 ± 12.12	44.62 ± 1.84	64.95 ± 2.62	108.47 ± 3.67	97.47 ± 3.39	45.74 ± 2.6	108.02 ± 4.10
Bi-214	1,120.29	287.53 ± 20.37	46.83 ± 2.38	62.69 ± 3.84	104.95 ± 6.23	94.85 ± 6.08	44.64 ± 3.08	109.79 ± 8.71
Pb-212	238.63	564.91 ± 29.32	65.32 ± 2.65	82.79 ± 5.34	103.44 ± 2.47	116.76 ± 3.96	67.55 ± 3.63	133.58 ± 4.95
Ac-228	338.4	533.93 ± 31.98	55.30 ± 2.08	112.85 ± 6.16	132.55 ± 5.14	130.89 ± 4.15	93.28 ± 6.12	111.88 ± 7.88
Ac-228	911.07	595.16 ± 42.85	70.32 ± 4.2	91.00 ± 6.09	138.64 ± 5.38	140.55 ± 5.38	88.55 ± 5.88	162.42 ± 13.28
Ac-228	968.9	626.93 ± 56.23	69.11 ± 5.23	96.74 ± 7.12	115.54 ± 7.64	122.49 ± 4.27	76.78 ± 5.91	139.03 ± 13.62
Tl-208	583.1	474.36 ± 29.81	59.39 ± 3.54	85.01 ± 5.51	119.36 ± 4.28	127.09 ± 5.14	86.11 ± 5.64	157.06 ± 10.51
Tl-208	2,614.47	589.62 ± 25.32	58.50 ± 4.04	92.44 ± 6.84	128.68 ± 7.25	140.9 ± 7.45	74.18 ± 4.41	152.71 ± 14.85
K-40	1,460.75	488.61 ± 18.56	433.28 ± 19.48	511.53 ± 18.75	520.63 ± 21.11	527.47 ± 17.38	403.37 ± 18.21	407.88 ± 15.46

Table 4
Absorbed gamma dose rate ($\dot{D}$), annual effective dose rate equivalent (AEDRE), Ra equivalent and hazard indices (H_{ex} and H_{in}), and gamma activity concentration index (I_γ) for the seven black sand samples.

Sample	Activity concentration (Bq/Kg)			Absorbed gamma dose rate	AEDRE	Radium equ. dose (Ra_{eq})	External hazard index	Internal hazard index
	U-238	Th-232	K-40	$\dot{D}$ (nGy/h)	(μSv/y)	(Bq/kg)	H_{ex}	H_{in}
Sample 1	252.38 ± 34.3	579.84 ± 53.1	488.61 ± 23.1	497.81	612.31	1,119.17	3.02	3.7
Sample 2	49.83 ± 5.6	64.65 ± 6.1	433.28 ± 20.8	81.19	99.86	175.65	0.47	0.61
Sample 3	64.51 ± 4.1	89.76 ± 10.8	511.53 ± 22.6	106.84	131.41	232.26	0.63	0.80
Sample 4	107.46 ± 6.4	121.99 ± 12.8	520.63 ± 21.8	147.09	180.92	321.99	0.87	1.16
Sample 5	96.90 ± 4.9	128.10 ± 10.8	527.47 ± 23.1	146.31	179.97	320.70	0.87	1.12
Sample 6	45.11 ± 3.1	77.81 ± 9.8	403.36 ± 20.1	85.97	105.74	187.44	0.51	0.62
Sample 7	108.29 ± 6.6	137.34 ± 16.7	407.87 ± 20.2	152.37	187.42	336.10	0.91	1.20
Range	45.11 ± 3.1–252.38 ± 34.3	64.65 ± 6.1–579.84 ± 53.1	403.36 ± 20.1–527.47 ± 23.1	81.19–497.81	99.86–612.32	175.65–1,119.17	0.47–3.02	0.61–3.7
Average	111.24 ± 24.5	140.38 ± 21.7	474.68 ± 36.3	158.36	194.78	348.78	0.94	1.24

absorbed dose rate to effective dose received by an average adult and the outdoor occupancy factor (considering that people on average spend approximately 20% of their time outdoors), respectively, as reported by UNSCEAR 2000 [5].

By using the data on activity concentrations of nuclides from Table 3, the absorbed gamma dose rates of the analyzed black sand samples were calculated and found to vary from 81.19 nGy/h to 497.81 nGy/h, which is higher than the worldwide mean value of ≈59 nGy/h. Also, Table 4 shows that the absorbed dose rate due to naturally occurring radionuclides of ^{232}Th in each black sand sample is higher than that attributable to other radionuclides such as ^{238}U and ^{40}K. The results of the calculations are given in Table 4.

3.3.3. Radium equivalent (Ra_{eq}) calculation

The radium equivalent activity (Ra_{eq}) is a weighted sum of the activities of the ^{238}U, ^{232}Th, and ^{40}K radionuclides based on the assumption that 370 Bq/kg of ^{238}U, 259 Bq/kg of ^{232}Th, and 4,810 Bq/kg of ^{40}K produce the same gamma ray dose rate, as given by the following equation:

$$\text{Ra (Bq/kg)} = A_{Ra} + 1.43A_{Th} + 0.077A_{(K)} < 370 \quad (11)$$

The maximum value of Ra_{eq} must be less than 370 Bq/kg, which is equivalent to an annual dose rate of 1mSv/y; this meets the maximum permissible dose to humans from their exposure to natural radiation from soil in 1 year.

The values of Ra_{eq} obtained for the collected black sand samples ranged from 175.65 Bq/kg to 1,119 Bq/kg; this range shows the lowest and the highest values, as shown in Table 4. The Ra_{eq} value of Sample 1 is much higher than the recommended value (<370 Bq/kg). As for the other samples, the Ra_{eq} values are satisfactory as per the recommendations, i.e., 175.65, 232.26, 321.99, 320.7, 187.44, and 336.1.

3.3.4. Internal hazard index, H_{in}

The internal hazard index (H_{in}) is used to control the internal exposure to ^{222}Rn and its radioactive progeny. It is given by the following equation [14,15]:

$$H_{ein} = \frac{A_{c(U)}}{185} + \frac{A_{c(Th)}}{259} + \frac{A_{c(K)}}{4810} \le 1 \quad (12)$$

If the maximum concentration of uranium in samples under investigation is half the normal acceptable limit, then the value of H_{in} will be less than 1. The calculated values of H_{in} (Table 4) were 3.7, 0.61, 0.8, 1.61, 1.12, 0.62, and 1.2. It should be noted that there is a significant difference in H_{in} for the seven samples. In the case of Samples 1, 4, 5, and 7, elevated values of H_{in} (i.e., 3.7, 1.61, 1.12 and 1.2, respectively), which are higher than the acceptable values, were observed. This is attributable to the high activity concentrations of gamma rays emitted from the daughter nuclides of both uranium and thorium. As for Samples 2, 3, and 6, the values of H_{in} are satisfactory (<1). The values were ~0.61, 0.8, and 0.62, respectively.

The annual effective dose rates of the analyzed black sand samples were found to range from 175.65 μSv/y to 1,119.17 μSv/y. These values are higher than the corresponding worldwide value of 80 μSv/y. This model takes into consideration the external hazard that is caused by γ-rays and that corresponds to a maximum radium equivalent activity of 370 Bq/kg for the samples. For the maximum value of H_{ex} to be less than unity, the maximum value of Ra_{eq} must be less than 370 Bq/kg. The external hazard index (H_{ex}) values, as determined from the analyzed samples, were 3.02, 0.47, 0.63, 0.87, 0.87, 0.51, and 0.91. The second to the last values (for H_{ex}) were within the acceptable worldwide mean range recommended by UNSCEAR, i.e., $H_{ex} < 1$. The highest value of H_{ex} (3.02) belongs to black sand Sample 1. This value is 3 times higher than the average range of the worldwide mean. This is attributable to the high activity concentration, particularly of the radionuclides of ^{232}Th and ^{40}K. The value $H_{ex} = 3.02$ indicates that the black sand from this location is a hazard concern and not recommended for use in building materials.

4. Conclusion

The black sand samples collected from Rashid city were nondestructively investigated and assayed using an HpGe detector and its associated electronics. The spectra due to the samples were collected and analyzed using Genie2000 software at the same geometry as the background and reference samples. The calculated MDA was found to be in a range of 0.03–0.73 Bq. The activity concentration values of the analyzed samples were in ranges from 64.65 ± 6.1 Bq/kg to 579.84 ± 53.1 Bq/kg for ^{232}Th, from 45.11 ± 3.1 Bq/kg to 252.38 ± 34.3 Bq/kg for ^{238}U, and from 403.36 ± 20.8 Bq/kg to 527.47 ± 23.1 Bq/kg for ^{40}K. The highest activity concentration values for the ^{238}U and ^{232}Th series were found to be 252.38 ± 34.3 Bq/kg and 579.84 ± 53.1 Bq/kg, respectively, in black sand Sample 1.

The radiation hazard Indices were calculated. It was observed that the absorbed gamma rose rates ranged from 81.19 nGy/h to 497.81 nGy/h, which is much higher than the worldwide mean value (59 nGy/h). The annual effective dose rates ranged from 99.86 μSv/yr to 612.31 μSv/yr, respectively. The external hazard indices (H_{ex}) resulting from these samples were 3.02, 0.47, 0.63, 0.87, 0.87, 0.51, and 0.91, respectively. The highest value (3.02) was found to belong to Sample 1, which has a value higher than the worldwide value (<1). The elevated results are mainly attributable to the high activity concentration of ^{232}Th and ^{40}K radionuclides in the analyzed black sand samples. It can be concluded that these samples should not be recommended for use as building materials;

their activities reflect the significant radiological hazard concern of the Rashid area. A comprehensive plan for the survey of this area is under investigation.

Conflict of interest

No conflicts, Rashid area of this study is a part of comprehensive study under investigation in the time being.

References

[1] G.R. Gilmore, Practical Gamma-ray Spectroscopy, second ed., John Wiley & Sons, New York, 2008, p. 408.
[2] IAEA, Thorium Fuel Cycle: Potential Benefits and Challenges, in IAEA-TECDOC, 1450, 2005.
[3] M. Abd El Wahab, H.A. El Nahas, Radionuclides measurements and mineralogical studies on beach sands, East Rosetta Estuary, Egypt, Chin. J. Geochem. 32 (2013) 146–156.
[4] A.W. Klement Jr. (Ed.), CRC Handbook of Environmental Radiation, CRC Press, Boca Raton, FL, 1982.
[5] C. Monty, UNSCEAR Report 2000: United Nations Scientific Committee on the effects of atomic radiation, sources and effects of ionizing radiation, J. Radiol. Protect. 21 (2001) 83.
[6] H. Cember, T. Johnson, Introduction to Health Physics, fourth ed., McGraw-Hill, New York, NY, 2008.
[7] S.F. Hassan, M.A.M. Mahmoud, M.A.E. Abd El-Rahman, Effect of radioactive minerals potentiality and primordial nuclei distribution on radiation exposure levels within muscovite granite, Wadi Nugrus, Southeastern Desert, Egypt, J. Geosci. Environ. Protect. 4 (2016) 62–78.
[8] D. Malain, P.H. Regan, D.A. Bradley, M. Matthews, T. Santawamaitre, H.A. Al-Sulaiti, Measurements of NORM in beach sand samples along the Andaman coast of Thailand after the 2004 tsunami, Nucl. Instrum. Methods Phys. Res. A 619 (2010) 441–445.
[9] M.R. Khattab, H. Tuovinen, J. Lehto, I.E. Al Assay, M.G. El Feky, M.A. Abd. El-Rahman, Determination of uranium in Egyptian graniteic ore by gamma, alpha, and mass spectrometry, Instrum. Sci. Technol. 45 (2017) 338–348.
[10] G.A. Dabbour, The Egyptian placer deposits — a potential source for nuclear raw materials, in: Proceedings of the Second Arab Conference on the Peaceful Uses of Atomic Energy, Cairo, 1994.
[11] J. Lilley, Nuclear Physics: Principles and Applications, J. Wiley & Sons, New York, 2001.
[12] A.G.E. Abbady, M.A.M. Uosif, A. El-Taher, Natural radioactivity and dose assessment for phosphate rocks from Wadi El-Mashash and El-Mahamid Mines, Egypt, J. Environ. Radioact. 84 (2005) 65–78.
[13] M. Tzortzis, H. Tsertos, S. Christofides, G. Christodoulides, Gamma-ray measurements of naturally occurring radioactive samples from Cyprus characteristic geological rocks, Radiat. Meas. 37 (2003) 221–229.
[14] Y. Örgün, N. Altinsoy, S.Y. Şahin, Y. Güngör, A.H. Gültekin, G. Karahan, Z. Karacik, Natural and anthropogenic radionuclides in rocks and beach sands from Ezine region (Çanakkale), Western Anatolia, Turkey, Appl. Radiat. Isot. 65 (2007) 739–747.
[15] S. Fares, A. Ashour, M. Abd El-Rahma, M. El-Ashry, Gamma radiation hazards and risks associated with wastes from granite rock cutting and polishing industries in Egypt, Yaderna ta Radyiatsyijna Bezpeka 1 (2012) 64–73.